


Capturing the Macroscopic Behaviour of Molecular Dynamics with Membership Functions

A. Sikorski ^{1,2}, R. J. Rabben ¹, S. Chewle ¹, and M. Weber ¹

¹Zuse Institute Berlin
²Free University of Berlin

07.06.2024*

Abstract

Markov processes serve as foundational models in many scientific disciplines, such as molecular dynamics, and their simulation forms a common basis for analysis. While simulations produce useful trajectories, obtaining macroscopic information directly from microstate data presents significant challenges. This paper addresses this gap by introducing the concept of membership functions being the macrostates themselves. We derive equations for the holding times of these macrostates and demonstrate their consistency with the classical definition. Furthermore, we discuss the application of the ISOKANN method for learning these quantities from simulation data. In addition, we present a novel method for extracting transition paths from simulations based on the ISOKANN results and demonstrate its efficacy by applying it to simulations of the μ -opioid receptor. With this approach we provide a new perspective on the analysis of macroscopic behaviour of Markov systems.

1 Introduction

Many physical processes are best understood as autonomous Markov processes (e.g., [8]). A common mathematical model for them are stochastic differential equations which allow to predict the probability for the future evolution of the system. Markovianity means, that this probability is just depending on the initial condition of the system. Solving the initial value problem is referred to as simulation of the system. The states of the generated trajectory are denoted as the micro states of the system.

As an illustration, consider the field of biomolecular system simulation [7]. Here a common mechanism being studied is the transformation of an inactive micro state of a receptor protein into an active state (by accordingly changing the coordinates of its atoms). The process can be mathematically modeled by the overdamped Langevin dynamics, a stochastic differential equation for the 3D coordinates of each atom in the protein and the solvent [6]. Typically these are analysed by simulation of the model, resulting in trajectories in a high-dimensional space.

However, often, the main focus of interest lies on the macro state behaviour of the system. A possible question to answer would be: What is the mean first passage time for an inactive receptor protein to become active? The two macro states in this regard are denoted as “inactive” versus “active”. At first glance, macro states S are subsets of the set of micro states Ω . In general, when given a starting set $S \subset \Omega$ of the system we want to know, how long on average the process stays in this set [20]. How long does a trajectory starting in the inactive

*Submitted to Proceedings of the Thematic Einstein Semester “Mathematical Optimization for Machine Learning”, de Gruyter

macro state remains there before leaving it, i.e. switching to the active macro state? The answer is given by the mean holding time $t_{\text{mh}}(\mathbf{x})$ defined by the integral:

$$t_{\text{mh}}(\mathbf{x}) = \int_0^{\infty} p_S(\mathbf{x}, t) dt.$$

where \mathbf{x} denotes the micro state of the system (the starting point $x(0) = \mathbf{x}$ of the trajectory) and the function $p_S(\mathbf{x}, t)$ denotes the probability that a trajectory is still in set S and has never left it during the whole time interval $[0, t]$. Formally $p_S(\mathbf{x}, t) = P_{\mathbf{x}}(T_S > t)$ is the holding probability of S conditioned on starting at the micro state \mathbf{x} with T_S being the first exit time of S . t_{mh} (also called mean first exit time) is then given by $t_{\text{mh}}(\mathbf{x}) = \mathbb{E}_{\mathbf{x}}[T_S]$.

If $t_{\text{mh}}(\mathbf{x})$ denotes the expected time until the system reacts, then

$$\mathbf{r}(\mathbf{x}) = -\nabla t_{\text{mh}}(\mathbf{x}) = -\nabla \int_0^{\infty} p_S(\mathbf{x}, t) dt$$

points into the direction where this time decreases the most. This can be seen as the micro-state-dependent reaction path direction $\mathbf{r}(\mathbf{x})$.

There is a conceptual problem now. We want to know the mean holding time for the macro state and not for every single micro state, but t_{mh} is a function of the micro states – the mean holding time in S depends on the starting point. Speaking of the “mean holding time of the macro state S ” would only make sense if it was independent of the micro-states position inside that macro state, i.e. if there was a set $S \subset \Omega$ and an exit rate $c_1 > 0$ allowing for a separation of the type

$$p_S(\mathbf{x}, t) = \mathbb{1}_S(\mathbf{x}) e^{-c_1 t}, \quad (1)$$

where $\mathbb{1}_S$ is the indicator function of the set S . In Markov State Modelling it is often asked for a decomposition of the state space Ω into subsets S which can be identified as “macro states” [11]. The separation approach (1) is a prerequisite for Markovianity of the macro state S and is approximately valid, if “leaving the set S ” is a very rare event compared to the mixing within S . The constant $c_1 > 0$ corresponds to the exit rate of S , because in this case $t_{\text{mh}}(\mathbf{x}) = \mathbb{1}_S(\mathbf{x}) \frac{1}{c_1}$ is independent of the choice of the starting point in S . This decomposition, however, is not possible in general and corresponds to instantaneous transitions which do not provide reaction paths inside S .

Classically the computation of (micro-state) mean holding times in the case of an S -based theory is provided by solving a partial differential equation [9]:

$$\mathcal{L}t_{\text{mh}}(\mathbf{x}) = -1,$$

for all $\mathbf{x} \in S$ with the boundary condition $t_{\text{mh}}(\mathbf{x}) = 0$ for all $\mathbf{x} \notin S$. In this equation the differential operator \mathcal{L} is the infinitesimal generator of the Koopmann operator of an autonomous Markov process and the equation essentially prescribes the mean holding time to decrease by one time unit per time unit until hitting the boundary. If the decomposition $t_{\text{mh}}(\mathbf{x}) = \mathbb{1}_S(\mathbf{x}) \frac{1}{c_1}$ were valid, then this equation would read

$$\mathcal{L}\mathbb{1}_S(\mathbf{x}) = -c_1 \mathbb{1}_S(\mathbf{x}). \quad (2)$$

Under the assumption of an ergodic system (e.g. for non-degenerate diffusion) the only set-based solutions are $S = \Omega$ with $c_1 = 0$ (the process never leaves Ω) or $S = \emptyset$. Clearly these trivial solutions are not of any use. How can we solve this conceptual problem?

When deriving exit rates for biomolecular processes, then the macro states of this system can not be rigorously described as subsets S in micro state space. Rather, transitions are gradual from something that is more inactive to something that can be described as more active. We propose replacing the indicator function $\mathbb{1}_S$ in (1) by a membership function $\chi : \Omega \rightarrow [0, 1]$ which quantifies how much a micro state $\mathbf{x} \in \Omega$ belongs to the starting macro state. The

theoretical background of our article, therefore, starts with the more general separation of space and time via

$$p_\chi(\mathbf{x}, t) = \chi(\mathbf{x}) e^{-c_1 t}. \quad (3)$$

By definition it satisfies the exponential decay of p_χ in t and at $t = 0$ the probability to be assigned to the starting state is given by χ . Therefore the χ functions with the smallest exit rates c_1 are the most persistent observables or measurements on the system satisfying Markovianity, i.e. time-homogeneous decay. Considering that, however defined, a macro state should be a function of the micro states and exhibit orderly, in our case Markovian, dynamics this gives rise to the fundamental idea of identifying the macrostate with the membership function: χ is the macro state and the macro state is given in and through χ . Generalising the classical set-based description to that by a χ -function allows us to obtain nontrivial macro-states which have proper exit-rates and therefore allow for a closed description of their dynamics. In this regard our ansatz can be seen as a necessary consequence of the demand for exact coarse-grained dynamics which is not possible with set-based decompositions.

At this point we have not provided a method to compute χ yet. χ can not be chosen arbitrarily. In order to preserve the Markovian long term behavior of the system a projection of the micro system to two different macro states has to be based on an invariant subspace of \mathcal{L} [19, 21]. Further requiring a decomposition into two complementary (i.e. such that they add up to one) macro states the simplest non-trivial solution is given by

$$\mathcal{L}\chi(\mathbf{x}) = -c_1\chi(\mathbf{x}) + c_2(1 - \chi(\mathbf{x})) \quad (4)$$

with $c_1, c_2 > 0$ and $\chi, 1 - \chi$ describing the two macrostates. These can be computed using PCCA+ [2] or ISOKANN [12, 16] and form an invariant subspace of \mathcal{L} which also guarantees long-term consistency with the original dynamics [21]. Whereas any solution to (4) leads to a dynamically closed macroscopic description, we will in general aim for solutions with small rates c_1, c_2 which represent temporally stable macro states.

In order to derive (4) one has to understand how the Markov property of a projected Markov process can be preserved. It means that projection and propagation of the system have to commute. Thus, the projection has to be based on an invariant subspace of \mathcal{L} . The constant function is an eigenfunction of \mathcal{L} . Thus a linear combination of a constant function and of a further eigenfunction leads to a feasible membership function χ . If we apply \mathcal{L} to such a linear combination, we arrive at (4). For the whole derivation we refer to [20].

In Section 2 of this paper we demonstrate that our macro state formalism based on the χ -function is consistent with the traditional set-based method: We show that when the χ -functions approach indicator functions the χ based equations reduce to the classical ones. We further motivate its physical meaning by giving a path-based interpretation of the resulting holding probabilities in terms of the Feynman-Kac formula.

In Section 3, we will suggest an approach to apply these theoretic results to extract transition paths from a set of given samples, before demonstrating its application to a molecular system given by the μ -opioid receptor in Section 4.

2 Theory of macroscopic exit rates

In the following, a consistent theory about macroscopic quantities based on a membership function $\chi : \Omega \rightarrow [0, 1]$ is derived. More precisely, the following quantities of interest are discussed:

- the definition of a macro state via $\chi(\mathbf{x})$,
- the corresponding position-independent exit rate c_1 ,
- the mean holding time $t_{\text{mh}}(\mathbf{x})$, and
- the reaction direction \mathbf{r} proportional to the gradient $-\nabla\chi$.

Note that computing reaction directions \mathbf{r} is possible for sets S , too, as described in the introduction. However, for sets we do not get this simple gradient form $-\nabla\chi$. The theory in this section is largely based on [20, 3]. We will extend the theory with statements about consistency and use it to support of the interpretation of χ as macro states, as explained in the introduction. The computation of χ will play an important role in our bio-molecular example, see section 4.

2.1 Defining macro states via membership functions

The starting point in the introduction is that $p_\chi = \chi e^{-c_1 t}$ would be a way to define holding times of macro states from a conceptual point of view to be able to interpret c_1 as an exit rate. The choice of χ is not arbitrary, but motivated by the necessity of an invariant subspace projection leading to (4). At this point it is not yet shown that p_χ when using the solution χ of (4) is consistent with the stochastic meaning of a holding probability. We will now demonstrate that it converges to the established definition if χ becomes the indicator function of a set.

We start by recalling some basic definitions. Let the state space Ω of a molecular system comprising N atoms be given as $\Omega = \mathbb{R}^{3N}$ where the position of each individual atom is described by three Cartesian coordinates. Let $\rho(\mathbf{x}, t) : \Omega \times \mathbb{R} \rightarrow [0, 1]$ denote the probability density distribution of states of the non-linear stochastic dynamics at time t . More precisely, the dynamics is given as a Markov process for which an infinitesimal generator $\mathcal{L}^* : L^1(\Omega) \rightarrow L^1(\Omega)$ (a differential operator, e.g. the Fokker-Planck operator) can be constructed that captures this time-dependent stochastic process. This operator is linear and describes the infinitesimal propagation of $\rho(\mathbf{x}, t)$:

$$(\mathcal{L}^* \rho)(\mathbf{x}, t) = \frac{d}{dt} \rho(\mathbf{x}, t). \quad (5)$$

It also gives rise to its adjoint generator $\mathcal{L} : L^\infty(\Omega) \rightarrow L^\infty(\Omega)$ which propagates observables instead of state densities. The partial differential equation (4) defining χ is formulated in terms of this adjoint. In this regard χ can also be interpreted as an observable, i.e. the measurement of the macro state. To allow for their interpretation as holding probability we are interested in solutions $\chi(\mathbf{x}) : \Omega \rightarrow [0, 1]$ with corresponding constants $c_1 > 0, c_2 > 0$.

Assume such χ and c_1, c_2 are given. We then define the χ -holding probability as

$$p_\chi(\mathbf{x}, t) := \chi(\mathbf{x}) e^{-c_1 t} \quad (6)$$

such that (4) becomes:

$$\mathcal{L}^* p_\chi = -c_1 p_\chi + c_2 p_\chi \frac{1 - \chi}{\chi}. \quad (7)$$

Rearranging results in:

$$\mathcal{L}^* p_\chi - c_2 p_\chi \frac{1 - \chi}{\chi} = -c_1 p_\chi. \quad (8)$$

Due to the relationship

$$\frac{\partial}{\partial t} p_\chi = \frac{\partial}{\partial t} \chi(\mathbf{x}) e^{-c_1 t} = -c_1 \chi(\mathbf{x}) e^{-c_1 t} = -c_1 p_\chi \quad (9)$$

Eq. (8) can also be represented as follows:

$$\mathcal{L}^* p_\chi - c_2 p_\chi \frac{1 - \chi}{\chi} = \frac{\partial}{\partial t} p_\chi. \quad (10)$$

The solution of the partial differential equation (10) together with the initial condition

$$p_\chi(\mathbf{x}, 0) = \chi(\mathbf{x}) e^{-c_1 \cdot 0} = \chi(\mathbf{x}) \quad (11)$$

can be given in terms of the Feynman-Kac formula [20, 3, 5]:

$$p_\chi(\mathbf{x}, \tau) = \mathbb{E} \left[\chi(\mathbf{x}_\tau) \cdot \exp \left(-c_2 \int_0^\tau \frac{1 - \chi(\mathbf{x}_t)}{\chi(\mathbf{x}_t)} dt \right) \middle| \mathbf{x}_0 = \mathbf{x} \right]. \quad (12)$$

This representation allows us to interpret the solution as an expectation over realizations of the stochastic process and therefore builds the bridge from an abstract definition to its interpretation as a probability.

To this end let us consider the case where $\chi \approx \mathbb{1}_S$. The expectation is to be taken over all trajectories starting in \mathbf{x}_0 . Once any such trajectory leaves the set S the integral becomes infinite and exponential function evaluates to 0. Otherwise the exponential stays 1, as well as $\chi(\mathbf{x}_\tau) = 1$. We therefore recover the definition of classical holding probability $p_\chi(\mathbf{x}, \tau) = p_S(\mathbf{x}, \tau)$ in (1), i.e. the probability to stay in S for time τ at least, see also (9) and (10) in [20], as well as (3.31) in [15].

We summarize this result in the following proposition:

Proposition 1. *Let $\chi \approx \mathbb{1}_S$ be a solution to (4). Then the χ -holding probability approximates the classical holding probability of S :*

$$p_\chi(\mathbf{x}, t) \approx p_S(\mathbf{x}, t).$$

With regard to this interpretation, $p_\chi(\mathbf{x}, t)$ is seen as the holding probability of the macro state χ . Due to the separated term $e^{-c_1 t}$ in (6), the holding probability decreases exponentially with the decay constant c_1 . This means that c_1 is the exit rate from χ . Since the function value of $p_\chi(\mathbf{x}, 0) = \chi(\mathbf{x})$ is interpreted as a holding probability, it is necessary that χ can only take values in the interval $[0, 1]$.

The time integral over the holding probability is the mean holding time $t_{\text{mh}}(\mathbf{x})$, which is proportional to the inverse of the exit rate c_1 :

$$t_{\text{mh}}(\mathbf{x}) = \int_0^\infty p_\chi(\mathbf{x}, t) dt = \int_0^\infty \chi(\mathbf{x}) e^{-c_1 t} dt = \lim_{t \rightarrow \infty} \left[-\frac{1}{c_1} \chi(\mathbf{x}) e^{-c_1 t} \right]_0^t = \frac{1}{c_1} \chi(\mathbf{x}). \quad (13)$$

The mean holding time immediately leads to a definition of a reaction direction: Following the gradient of t_{mh} increases the time until “a reaction takes place”. Therefore by defining the reaction direction $\mathbf{r} : \Omega \rightarrow \mathbb{R}^{3N}$,

$$\mathbf{r}(\mathbf{x}) = -\nabla t_{\text{mh}}(\mathbf{x}) = -\frac{1}{c_1} \nabla \chi(\mathbf{x}) \propto -\nabla \chi(\mathbf{x}), \quad (14)$$

we obtain a vector field along which the mean holding time decreases uniformly and which is proportional to $\nabla \chi$. This also means that χ itself can be understood as an order parameter, i.e. a reaction coordinate for the system. Note that we obtain this time independent result only as a consequence of the initial time separation ansatz for p_χ . By integrating curves tangential to \mathbf{r} one can obtain reaction paths in Ω . In Section 3 we will make use of the order parameter interpretation to subsample a representative reactive path from a given pool of simulation data.

The possibility of calculating these quantities of interest from (4) is a motivation to develop an efficient method for solving this equation. We will now show how to express these quantities in terms of the Koopman operator, before discussing ISOKANN, an algorithm for their computation.

2.2 Membership functions from Koopman operator

So far the description of χ was based on the infinitesimal generator \mathcal{L} but a suitable analytical solution of the corresponding partial differential equation (4) is not available. However, it is possible to transform (4) into an equation for which a constructive solution is possible. We will now show how we can similarly formulate it in terms of the Koopman operator \mathcal{K} and how we can switch between the formalisms and work out the relation between χ function and eigenfunctions of \mathcal{K}^τ . The problem of actually computing χ will then be addressed in the next subsection.

The Koopman operator \mathcal{K}^τ is the time-integral or solution operator of \mathcal{L}^* for some lag-time $\tau > 0$ and can be formally defined as $\mathcal{K}^\tau = e^{\tau\mathcal{L}^*}$. It can also be defined by its action on observable functions $f : \Omega \rightarrow \mathbb{R}$:

$$(\mathcal{K}^\tau f)(\mathbf{x}) := \mathbb{E}[f(x(\tau)) \mid x(0) = \mathbf{x}], \quad (15)$$

where the expectation is taken over independent realizations x of the process, starting in $x(0) = \mathbf{x}$. It can be understood as the expected measurement $\mathcal{K}^\tau f$ of an observable f after a lag time τ . Being an expectation value its action can be approximated using Monte-Carlo estimates over simulations, making it particularly suitable for applications.

To transform (4) into an equation for \mathcal{K}^τ we substitute

$$\alpha = c_1 + c_2 \quad (16)$$

to arrive at the following equation:

$$\mathcal{L}^* \chi = -\alpha \chi + c_2. \quad (17)$$

This shows that \mathcal{L} acts as a shift-scale operator on χ if and only if χ solves (4). Making use of the formal exponential representation of \mathcal{K}^τ and its series expansion one obtains [20, 3]:

$$\mathcal{K}^\tau \chi = e^{-\tau\alpha} \chi + \frac{c_2}{\alpha} (1 - e^{-\tau\alpha}). \quad (18)$$

Setting

$$\gamma_1 = e^{-\tau\alpha}, \quad \gamma_2 = \frac{c_2}{\alpha} (1 - \gamma_1) \quad (19)$$

this becomes:

$$\mathcal{K}^\tau \chi = \gamma_1 \chi + \gamma_2. \quad (20)$$

So, just as with equation (17), \mathcal{K}^τ acts as a shift-scale if and only if χ is a solution to (4). Noting that $\mathcal{K}^\tau \mathbb{1} = \mathbb{1}$ we further see that $f := \chi - \frac{c_2}{\alpha}$ is an eigenfunction of \mathcal{K}^τ with eigenvalue γ_1 :

$$\mathcal{K}^\tau \left(\chi - \frac{c_2}{\alpha} \right) = \gamma_1 \chi + \frac{c_2}{\alpha} (1 - \gamma_1) - \frac{c_2}{\alpha} = \gamma_1 \left(\chi - \frac{c_2}{\alpha} \right). \quad (21)$$

These findings are summarized in the following proposition:

Proposition 2. *Let the parameters $c_1, c_2, \alpha, \gamma_1, \gamma_2$ satisfy their relations above. The following are equivalent:*

- χ solves the ISOKANN problem (4).
- \mathcal{L} acts as a shift-scale on χ with scale $-\alpha$ and shift c_2 .
- \mathcal{K}^τ acts as a shift-scale on χ with scale γ_1 and shift γ_2 .
- $\chi - \frac{c_2}{\alpha}$ is an eigenfunction of \mathcal{K}^τ with eigenvalue γ_1 .

The above identities allow us to switch between the infinitesimal generator and Koopman framework. In particular, we can compute the exit rate c_1 from the Koopman parameters γ_1 and γ_2 :

$$\alpha = -\frac{\ln \gamma_1}{\tau}, \quad c_2 = \frac{\alpha \gamma_2}{1 - \gamma_1}, \quad c_1 = \alpha - c_2. \quad (22)$$

This allows to estimate the respective constants, e.g. the exit rate c_1 , by evaluating χ and $\mathcal{K}^\tau \chi$ at sample points $\mathbf{x} \in \Omega$ and solving the linear regression problem (20).

2.3 ISOKANN for computing membership functions

The ISOKANN (Invariant subspaces of Koopman operators learned by a neural network) method [12, 17, 16] is a fixed-point iteration which combines the use of a neural network for representing the high-dimensional χ function with the Koopman formalism to enable its training on simulation data.

On convergence it returns χ that solves (4), (17) and (20). Solving the partial differential equations involving \mathcal{L}^* directly is not feasible due to the high dimensionality of molecular systems. Molecular simulations on the other hand enable us to estimate the action of \mathcal{K}^τ on an observable. For this reason, ISOKANN attempts to solve (20) by using the action of \mathcal{K}^τ for the calculation of $(\mathcal{K}^\tau \chi_i)(\mathbf{x})$, where χ_i is the i -th iterate of χ and \mathbf{x} is a training point. It approximates the expectation value

$$(\mathcal{K}^\tau \chi_i)(\mathbf{x}) := \mathbb{E}[\chi_i(x(\tau)) \mid x(0) = \mathbf{x}], \quad (23)$$

by a Monte-Carlo estimate over trajectory simulations x starting in different starting points \mathbf{x} . The next iterate is then given by the shift-scaled $\mathcal{K}^\tau \chi_i$:

$$\chi_{i+1} := \frac{\mathcal{K}^\tau \chi_i - \min(\mathcal{K}^\tau \chi_i)}{\|\mathcal{K}^\tau \chi_i - \min(\mathcal{K}^\tau \chi_i)\|_\infty}, \quad (24)$$

which is motivated by inverting the shift and scale of (20), such that the solution χ to (20) is indeed a fixed point. The initial guess χ_0 is chosen randomly. ISOKANN is based on the power method, an iterative method used to obtain the dominant eigenfunction of a linear operator. In ISOKANN additional scaling and shifting in each iteration ensures that it does not converge to the constant function, but against the membership function $\chi(\mathbf{x}) : \Omega \rightarrow [0, 1]$ [17] – similar to targeting the second eigenvalue in the inverse power method. In order to represent the iterates χ_i , we approximate them by a neural network. The equality assignment in the iteration (24) thus becomes a supervised learning problem at data points \mathbf{x} with labels given by the corresponding right hand side of (24) evaluated on the previous generation of the network. The iterations are then terminated by a stopping criterion which can be either a high correlation coefficient $(\chi_i(\mathbf{x}_n), \chi_{i+1}(\mathbf{x}_n))_n$ or a small empirical loss $\|\chi_i - \chi_{i+1}\|_2$, indicating that we found an approximate solution to (20).

Assuming infinite data and perfect representation by the neural network, this iteration indeed converges to the solution χ of (20)[17] with the smallest rate c_1 . It is spanned by the constant eigenfunction with eigenvalue 0 and the second eigenfunction with eigenvalue closest to 0. This solution is unique, if the corresponding eigenvalue is simple. In practice however, for a cluster of low-lying eigenvalues, this routine can result close to one of multiple possible membership functions (each representing one of these slower processes). In that case the procedure can be repeated and the resulting membership functions can be used to construct an invariant subspace of \mathcal{K} .

One of ISOKANN’s main benefits is that it avoids discretizing the state space, which is crucial for the application to high-dimensional systems and avoiding the curse of dimensionality [12]. In the ISOKANN algorithm it is possible to train artificial neural networks by collecting many short-term trajectories of simulation length τ from different starting points in high-dimensional spaces. Thus, ISOKANN can be applied to many independent short-time trajectories or it can even decide where in Ω to enrich simulation data [17]. In our illustrative example we will apply it to a small number of medium-length trajectories. The resulting χ function will then be used to subsample a reactive path from the data, which leads us to the next section.

3 Extracting transition paths from simulations

Once we obtained a χ function from ISOKANN we might be tempted to directly compute a reaction path following the gradient of χ as in (14). This however is problematic as the neural network approximation is good only in the region of sufficient training data. The gradient of χ however could point away from this region, accumulating more and more approximation errors

and quickly lead to unobserved unphysical states. One might solve this problem by projecting back to the physical regime, e.g. via energy minimization. This however requires access to the original systems potential/forces and is not only computationally expensive but also involved from an implementation perspective.

We now propose an alternative method which can be applied as a post-processing step to already sampled simulation data without requiring further information about the system. Applied as a post-processing step to molecular simulations, together with ISOKANN, it provides researchers with a direct step-by-step representation of the slowest process (which is contained in the simulation data) by identifying this process and filtering out the intermediate fluctuations.

To this end we understand the learned χ values as an order parameter for a set of simulation data in Ω . As shown in (13), the membership values are interpreted to be proportional to mean holding times of a macro state. The level sets of the function $\chi(\mathbf{x})$ in this regard correspond to micro states \mathbf{x} which “take place simultaneously” in this newly defined time axis. By interpreting this mean-holding-time as a “temporal” parameter we can extract macroscopic transition paths from simulation data. Replacing the time from the simulation by χ furthermore allows us to incorporate data of different simulations, treating them merely as χ ordered data points and thus allowing for higher resolution of the results.

The core problem of choosing a path through the data samples consists of balancing the progress in the reaction direction, $\nabla\chi$, versus spatial movement on the levelsets of χ . More formally we look for an ordered list $I \subset J = \{1, \dots, N\}$ of samples from simulation points $X_J = (\mathbf{x}_j)_{j \in J}$ in Ω , such that $\chi(\mathbf{x}_j)$ is an increasing sequence with smooth spatial transitions, i.e. without large deviations $\mathbf{x}_{j+1} - \mathbf{x}_j$. To this end we will model the spatial movement as a Brownian motion through the time-parameter χ .

For the classical Brownian motion $dX_t = \sigma dW_t$ the probability of obtaining a specific set of samples, conditioned on the sampling time points t_i , is given by the finite dimensional distribution [9] (in our case we assume $\mathbf{b} \equiv 0$ and $\sigma(\mathbf{x}) \equiv \sigma$ as well as $t = \chi$):

$$p(\mathbf{x}_1, \dots, \mathbf{x}_n | t_1, \dots, t_n) = \left(\prod_{i=1}^{n-1} (2\pi\sigma^2\Delta t_i)^{-d/2} \right) \exp \left(- \sum_{i=1}^{n-1} \frac{\|\mathbf{x}_{i+1} - \mathbf{x}_i\|^2}{2\sigma^2\Delta t_i} \right). \quad (25)$$

This formula is typically used to obtain the probability given a specific set of $\Delta t_i = t_{i+1} - t_i$. In our case we will use it to also compare different sampling times t_i by setting $p(\mathbf{x}_1, \dots, \mathbf{x}_n | t_1, \dots, t_n) = p(\mathbf{x}_1, \dots, \mathbf{x}_n, t_1, \dots, t_n)$ which allows to balance temporal with spatial jumps. This can be justified from a Bayesian perspective as prescribing a uniform prior on the number and length of time intervals (as we have no preference for specific Δt values to appear in the solution) although further investigation of this view may be warranted. The parameter σ plays the role of a smoothing parameter, balancing the likelihood of jumps in space or time. A high σ allows for more erratic jumps over short time-spans while a lower σ favors spatially closer jumps possibly necessitating longer time-spans, as illustrated in Figure 1.

We now continue to find the maximum likelihood path through our sampling data by replacing the classical time parameter with the samples χ value, such that $\Delta t_i = \chi(x_{i+1}) - \chi(x_i)$.

Taking the logarithm allows us to transform (25) into a sum of log probabilities, $\log p(\mathbf{x}_1, \dots, \mathbf{x}_n) = \sum_{i=1}^n \log p(\mathbf{x}_i, \mathbf{x}_{i+1})$ with

$$\log p(\mathbf{x}, \mathbf{y}) = \log \left((2\pi\sigma^2 (\chi(\mathbf{y}) - \chi(\mathbf{x})))^{-d/2} \right) - \frac{\|\mathbf{y} - \mathbf{x}\|^2}{2\sigma^2(\chi(\mathbf{y}) - \chi(\mathbf{x}))}. \quad (26)$$

Finding the maximal likelihood path then corresponds to solving the shortest path problem from a (set of) point(s) $\chi(\mathbf{x}_i) \approx 0$ to a (set of) point(s) $\chi(\mathbf{x}_i) \approx 1$ with edge distance e_{ij} between two points (nodes)

$$e_{ij} = \begin{cases} -\log p(\mathbf{x}_i, \mathbf{x}_j) & \text{if } \chi(\mathbf{x}_i) < \chi(\mathbf{x}_j) \\ \infty & \text{otherwise,} \end{cases} \quad (27)$$

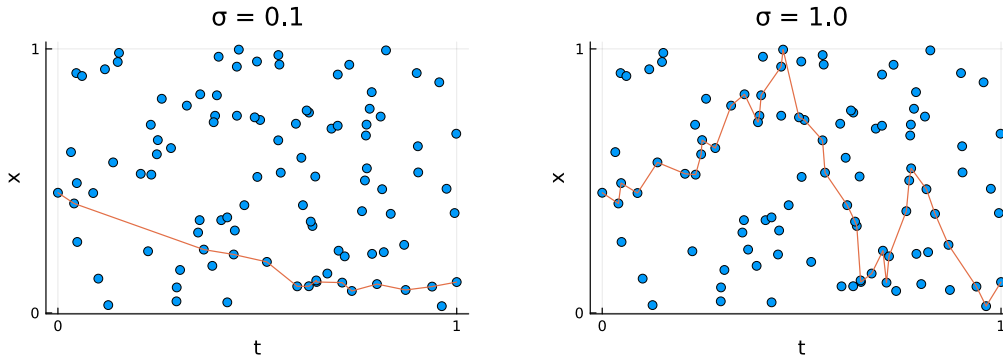


Figure 1: Illustration of the maximum likelihood path (25) on 100 points distributed uniformly in space and time. For lower σ values (left) the path prefers less jumps with small spatial displacement, whilst for higher σ (right) the path goes through more points at the cost of more erratic movement. Note that this is just an illustration of the maximum-likelihood-path with synthetic data in classical time t (which in our application will be replaced by χ).

where transitions forward in time (i.e. increasing χ -value) are enforced by the corresponding ∞ weight. The shortest path problem can be solved with the Bellman-Ford algorithm [4].

Of course the assumption of uniform Brownian motion for the underlying dynamics is far-fetched for an actual molecular system. However, with only finite simulation data, the locally possible jumps will be dictated mainly by the available data which already incorporates the physical drift. The Brownian assumption introduces only a small bias which is largely negligible for the choice of paths in the temporal, i.e. χ direction, as any larger deviations from the Brownian distribution will already be reflected in the available data. We believe this can be improved in cases where the acceleration (force and masses) and the diffusion coefficient σ of the dynamics are known. This however is not straightforward, as we have replaced the ordinary time with χ which requires some projection of the stochastic process.

In this regard our proposed algorithm can be understood as a simple heuristic filtering method to obtain a smooth path through already provided samples along the learned reaction coordinate from $\chi = 0$ to $\chi = 1$ (or vice versa). The result is the most-likely path (under the Brownian assumption) between the extremal conformations identified by χ . Being composed of the actually simulated, hence physically relevant, data it provides a smooth transition through the identified slowest process indexed by the mean holding time of the corresponding macro-state.

4 Illustrative Example: Opioid Receptor

To illustrate the added value of χ computation, we will show an molecular dynamics (MD) example which is part of a pharmaceutical project. We first learned the χ function from molecular simulation trajectories and applied the described reaction path extraction along χ to a high-dimensional molecular system consisting of 4734 atoms. The application background is given by understanding pain relief using opioids. Strong painkillers like morphine and fentanyl act upon a special type of receptor in the body known as the μ -opioid receptor (MOR). This receptor is part of the family of opioid receptors and is a G-protein coupled receptor found in various parts of the body such as brain, spinal chord, and gastrointestinal tract [10]. The indiscriminate activation of the MOR across the whole body is one of the causes of severe side-effects of this family of strong pain killers. [1].

However, it is proven that chemical changes at site of inflammation cause the creation of a micro-environment [13]. The knowledge about the local micro-environment can be used to design peripherally restricted strong pain killers with potentially less side-effects [18]. Different micro-environments may lead to different dynamics of the MOR. One possible chemical change of the MOR in inflamed tissue postulates the formation of disulfide bonds as the concentration

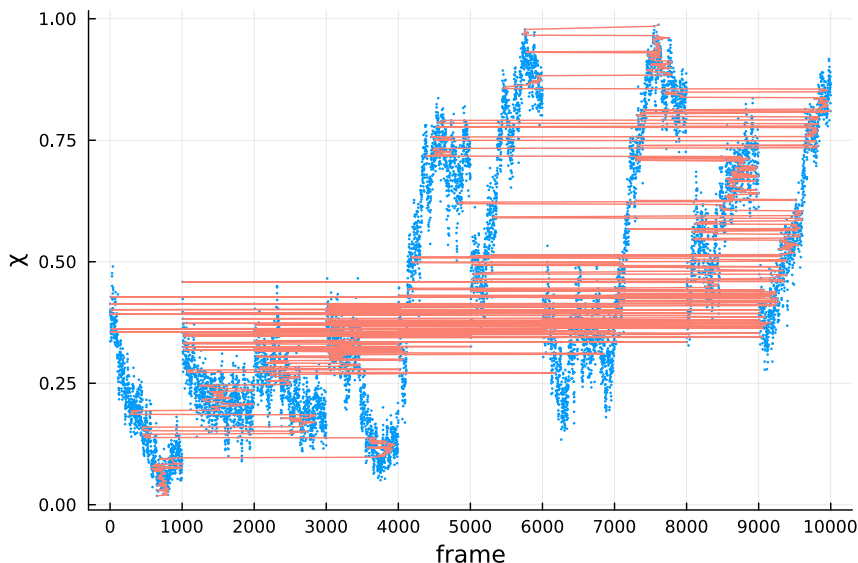


Figure 2: The membership value $\chi(x)$ for each state (frame) x obtained from 10 independent simulations, with each simulation comprising 1,000 frames. The y-axis represents the macroscopic transition, showing that different trajectories cover distinct segments of this transition while exhibiting partial overlap with other trajectories. The extracted reaction path (orange line) progresses monotonously from $\chi \approx 0$ to $\chi \approx 1$ while maintaining (not depicted) spatially smooth transitions. Note that it incorporates the data from amongst all 10 simulations and even jumps between them where facilitated by small spatial distances in Ω .

of reactive oxygens species goes up.

4.1 Algorithmic details

Our input data is taken from 10 different simulations of the MOR. After the primary proximity analysis on the active structure of the MOR (Protein Data Bank (PDB) ID 8EF5) a disulfide bond was introduced in the inactive structure of the MOR in between location CYS159 and CYS251 (Protein Data Bank ID 7UL4) [22, 14]. 10 simulations (with explicit water and with a lipid-bilayer for the MOR) were run. Each simulation spans an interval of 100 nanoseconds, totalling to 1 microsecond.

After simulation, pairwise distances over all α -carbons that can be observed to be closer than a threshold ($d_{\max} = 12 \text{ \AA}$) at least once over the simulation time (normalized to mean 0 and standard deviation 1) serve as input features of the corresponding neural network of the ISOKANN algorithm [16]. The action of the Koopman operator in (24) is estimated with one sample each forward and backward along the time axis, justified by the reversibility of the system. This is used to train the χ -function. With taking forward and backward steps, it is avoided that χ has all its mass in the terminal point. An uni-directed trajectory, i.e. if only forward or only backward steps were taken, would “transport” the χ values along the trajectory to the final point in the estimation of the Koopman operator: The Koopman estimation of each point in (24) would simply be the χ value at the trajectories predecessors point. Over time all points would attain the value of the first point, whereas the shift-scale would enforce the last point to remain distinct.

The neural network is a multilayer perceptron with 3 fully connected hidden layers of size (6161, 336, 18) with sigmoid activation functions and a single linear output neuron. For the optimisation we use ADAM with a learning-rate of $\eta = 1e-4$ with a $L2$ regularization of $\lambda = 1e-2$ and a minibatch-size of 128. After training χ for 30,000 iterations we concluded convergence based on the plateauing of the mean squared error of the ISOKANN residuals at around $5e-4$. The described shortest path is extracted with $\sigma = 0.7$ resulting in 1,231 selected

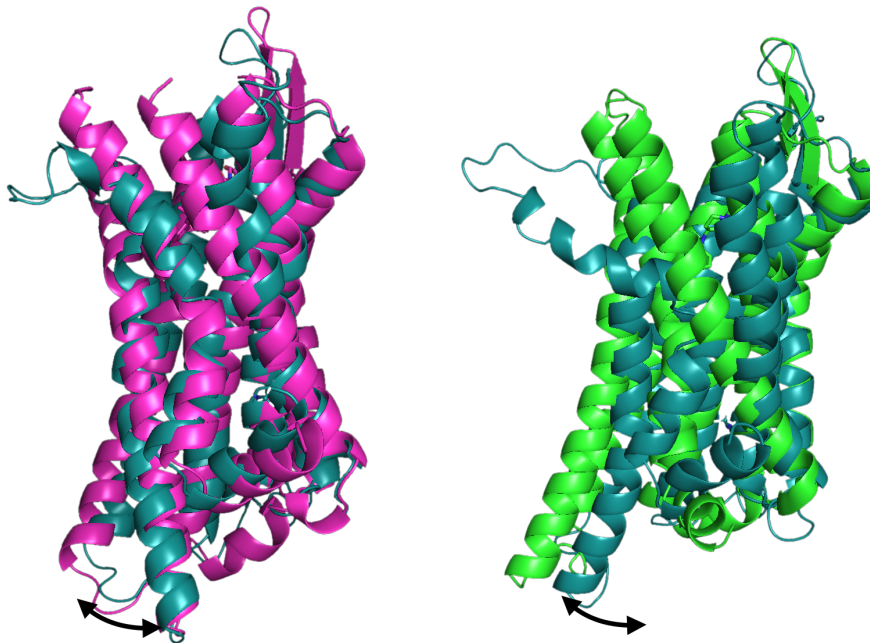


Figure 3: Visualization of the MOR states (teal) at the beginning (left) and end (right) of the transition path from figure Fig. 2 (orange). The superimposed purple and green structures are known to be representative of the inactive (PDB 7UL4) resp. active (PDB 8EF5) states. We can see that ISOKANN isolates close similar to these known metastabilities from the simulation trajectories without their a priori knowledge. The reactive path clearly displays the tilting motion (black arrow) undergone by the transmembrane helix 6.

frames.

Using a large regularization for the neural network enforces a smooth structure to the χ function which may also be understood as a smoothing of the data and thereby artificially connecting spatially adjacent samples. With regularization ISOKANN, thus, isolates the spatially large transitions which amount to macroscopic changes.

4.2 Application to MOR

ISOKANN serves as an efficient tool to analyse rare events in the simulation of the μ -opioid receptor. As mentioned earlier, finding a solution function χ of (20) with a low exit rate c_1 corresponds to the identification of a “reaction coordinate”. In Fig. 2 the resulting χ -values along 10 independent molecular simulations are shown (blue dots). One can see that the lowest and highest values of χ are not to be found within one trajectory. Using ISOKANN, it is possible to extract the “dynamically most distant” frames from the simulation, see Fig. 3. Indeed the χ -values correspond to a reaction coordinate for the transition from an inactive to an active macro state of MOR. Although none of the 10 trajectories simulates this process completely, we can extract the time-determining steps along the reaction path by using the shortest path routine described in section 3. The picked path is rather small in length (1,231 frames, orange in Fig. 2) as compared to entire trajectory of 10,000 stored frames. It displays a physically plausible and compellingly smooth transition between the extremal states.

Whereas it was not at all clear whether the supplied simulation data was sufficient a priori, the resulting path identifies the known crystal structures and a path between them. Fig. 3 displays the modified MOR (teal) with a disulfide bond at the starting point of the reaction path aligning with the inactive structure of the unmodified, natural state of the MOR (purple). Laboratory experiments suggest partial activation of the MOR which is confirmed by the shortest path analysis in the tilting movement of the transmembrane helix 6 (bottom left) outwards like it is seen in the fully activated, natural MOR crystal structure (green). It’s

noteworthy that the start and end points of the reactive path were determined without prior knowledge of the crystal structures. Extracting these extremal states and the transition path from the raw trajectory data frame-by-frame would pose a considerable challenge.

Using a linear regression to estimate γ_1, γ_2 in (20) we can compute the exit rate for a given lag time $\tau = 0.1$ ns by (22) resulting in $c_1 \approx 0.06$ ns⁻¹.

5 Conclusion

In bridging the conceptual gap between microstate and macrostate analyses, we introduced the notion of mean holding probabilities $p_\chi(\mathbf{x}, t) = \chi(\mathbf{x})e^{-c_1 t}$ represented in terms of membership functions χ which we interpret as the macrostate itself. Taking this as a theoretical starting point, the computation of mean holding times $t_{mh} \propto \chi$, which generalize their classical set-based definitions, and of reaction paths along $\mathbf{r} \propto -\nabla\chi$ has been shown. Being proportional to a mean holding time, $\chi(\mathbf{x})$ represents a kind of temporal order of micro states $\mathbf{x} \in \Omega$ in a high-dimensional space Ω thereby serving as a reaction coordinate.

We briefly described ISOKANN, a machine-learning-based algorithm, which we use to approximately solve the high-dimensional partial differential equation (4) defining χ . In a further step we interpret the values of the obtained solution χ to define the weights of edges of a graph, in which the vertices represent biomolecular micro states of an opioid-receptor simulation. Solving a shortest path problem for this graph allows us to obtain a subsample of the simulation data which captures the time-determining steps of macro molecular transitions.

Our method is able to pick micro states from different independent MD trajectories generated for the same biomolecular system in order to combine them into one “temporally and spatially” ordered path between macro states, see Fig. 2. This path shows the time-determining steps of a rare transition event between the macro states.

In our example, this approach effectively condenses 10,000 frames into a concise set of 1,231 frames. Using ISOKANN together with shortest path computation extracts what “really is to be seen” in the trajectories. In this case, the extracted path accurately depicts the transition of the modified MOR from an inactive to an active state as also indicated in experimental conditions. It further enhances our understanding of the role of a disulfide bond resulting from oxidative stress. Supported by this findings detailed experiments highlighting the role of implicated cysteins pair (159 and 251) out of other 2 pairs are planned. This example highlights ISOKANN’s potential to significantly streamline the analysis of long-term MD simulations and extract meaningful reaction paths.

Acknowledgement

The research of A. Sikorski was funded by the DFG through the CRC 1114 “Scaling Cascades in Complex Systems” (project B03). The research of R. J. Rabben was funded by the NHR Graduate School of the NHR Alliance. The research of S. Chewle was funded by the BMBF through the project CCMAI (funding code 01GQ2109A).

References

- [1] E. Darcq and B. L. Kieffer. Opioid receptors: drivers to addiction? Nature Reviews Neuroscience, 19(8):499–514, 2018.
- [2] P. Deuffhard and M. Weber. Robust Perron Cluster Analysis in Conformation Dynamics. Linear Algebra and its Applications, 398c:161–184, 2005.
- [3] N. Ernst, K. Fackeldey, A. Volkamer, O. Opatz, and M. Weber. Computation of temperature-dependent dissociation rates of metastable protein–ligand complexes. Molecular Simulation, 45(11):904–911, 2019.
- [4] L. R. Ford. Network flow theory. Rand Corporation Santa Monica, CA, 1956.

- [5] H. Gzyl. The Feynman-Kac formula and the Hamilton-Jacobi equation. Journal of Mathematical Analysis and Applications, 142(1):74–82, 1989.
- [6] B. Leimkuhler and C. Matthews. Molecular Dynamics: With Deterministic and Stochastic Numerical Methods, volume 39 of Interdisciplinary Applied Mathematics. Springer International Publishing and Imprint: Springer, Cham, 1st ed. 2015 edition, 2015.
- [7] C. Mura and C. E. McAnany. An introduction to biomolecular simulations and docking. Molecular Simulation, 40(10–11):732–764, Aug. 2014.
- [8] J. R. Norris. Markov chains, volume 2 of Cambridge series on statistical and probabilistic mathematics. Cambridge University Press, Cambridge, 1998.
- [9] G. A. Pavliotis. Stochastic Processes and Applications – Diffusion Processes, the Fokker-Planck and Langevin Equations. Springer, 2014.
- [10] C. B. Pert and S. H. Snyder. Opiate receptor: demonstration in nervous tissue. Science, 179(4077):1011–1014, 1973.
- [11] J. Prinz, H. Wu, M. Sarich, B. Keller, M. Senne, M. Held, J. Chodera, C. Schütte, and F. Noé. Markov models of molecular kinetics: Generation and validation. J Chem Phys., 134(17):174105, 2011.
- [12] R. J. Rabben, S. Ray, and M. Weber. ISOKANN: Invariant subspaces of Koopman operators learned by a neural network. The Journal of Chemical Physics, 153(11):114109, 2020.
- [13] P. W. Reeh and K. H. Steen. Tissue acidosis in nociception and pain. Progress in brain research, 113:143–151, 1996.
- [14] M. J. Robertson, M. M. Papasergi-Scott, F. He, A. B. Seven, J. G. Meyerowitz, O. Panova, M. C. Peroto, T. Che, and G. Skiniotis. Structure determination of inactive-state gpcrs with a universal nanobody. Nature Structural & Molecular Biology, 29(12):1188–1195, 2022.
- [15] C. Schütte, S. Klus, and C. Hartmann. Overcoming the timescale barrier in molecular dynamics: Transfer operators, variational principles and machine learning. Acta Numerica, 32:517–673, 2023.
- [16] A. Sikorski. Julia Package: ISOKANN.jl. <https://github.com/axsk/ISOKANN.jl>, 2023.
- [17] A. Sikorski, E. Ribera Borrell, and M. Weber. Learning Koopman eigenfunctions of stochastic diffusions with optimal importance sampling and ISOKANN. Journal of Mathematical Physics, 65(1):013502, 01 2024.
- [18] V. Spahn, G. Del Vecchio, D. Labuz, A. Rodriguez-Gaztelumendi, N. Massaly, J. Temp, V. Durmaz, P. Sabri, M. Reidelbach, H. Machelska, M. Weber, and C. Stein. A nontoxic pain killer designed by modeling of pathological receptor conformations. Science (New York, N.Y.), 355(6328):966–969, 2017.
- [19] M. Weber. A Subspace Approach to Molecular Markov State Models via a New Infinitesimal Generator. Habilitation thesis, FU Berlin, 2011.
- [20] M. Weber and N. Ernst. A fuzzy-set theoretical framework for computing exit rates of rare events in potential-driven diffusion processes, 2017.
- [21] M. Weber and S. Kube. Preserving the Markov Property of Reduced Reversible Markov Chains. In T. E. Simos and C. Tsitouras, editors, Numerical Analysis and Applied Mathematics: International Conference on Numerical Analysis and Applied Mathematics 2008, volume 1048 of American Institute of Physics Conference Series, pages 593–596, Sept. 2008.

- [22] Y. Zhuang, Y. Wang, B. He, X. He, X. E. Zhou, S. Guo, Q. Rao, J. Yang, J. Liu, Q. Zhou, et al. Molecular recognition of morphine and fentanyl by the human μ -opioid receptor. Cell, 185(23):4361–4375, 2022.